The influence of conformational changes in a miR122-dependent long-range interaction between hepatitis C virus 5' non-coding and core-encoding regions

Kirsten Bentley Corresp., [1] , **Jonathan P Cook** [2] , **Andrew K Tuplin** [3] , **David J Evans** [1]

[1] BSRC and School of Biology, University of St Andrews, St Andrews, United Kingdom
[2] School of Life Sciences, University of Warwick, Coventry, United Kingdom
[3] The Faculty of Biological Sciences, University of Leeds, Leeds, United Kingdom

Corresponding Author: Kirsten Bentley
Email address: kb209@st-andrews.ac.uk

The hepatitis C virus RNA genome possesses a variety of conserved structural elements, in both coding and non-coding regions, that are important for viral replication. Some of these elements are known or predicted to modulate key life cycle events, such as translation and genome replication, involving conformational changes induced by long-range RNA-RNA interactions. One such element is SLVI, a stem-loop (SL) structure located towards the 5' end of the core protein-coding region. This element is predicted to form an alternative RNA-RNA interaction with complementary sequences in the 5'UTR that are themselves involved in the binding of the cellular microRNA 122 (miR122). The switch between ‘open’ and ‘closed’ structures involving SLVI has previously been suggested to modulate translation, with lower translation efficiency associated with the ‘closed’ conformation. In the current study, we have used selective 2'-hydroxyl acylation analysed by primer extension (SHAPE) to validate this RNA-RNA interaction in the absence and presence of miR122. Using site-directed mutations introduced to promote one or other conformation we have found no correlation between the predicted structural conformation and translation enhancement. In addition, we observed no influence on replication compared to wild type, indicating that favouring ‘open’ or ‘closed’ interactions also does not unduly alter virus replication. Overall, our data suggests that while SLVI may undergo structural re-arrangements involving a switch from ‘open’ to ‘closed’ conformations this has limited phenotypic effect.

The influence of conformational changes in a miR122-dependent long-range association between hepatitis C virus 5' non-coding and core-encoding regions.

Kirsten Bentley[1*], Jonathan Cook[2], Andrew Tuplin[3] and David J. Evans[1]

Affiliations:

[1] BSRC and School of Biology, North Haugh, University of St Andrews, Fife, UK.

[2] School of Life Sciences, University of Warwick, Coventry, UK.

[3] The Faculty of Biological Sciences, University of Leeds, Leeds, UK.

[*] Communicating author: Kirsten Bentley, kb209@st-andrews.ac.uk.

Abstract

The hepatitis C virus RNA genome possesses a variety of conserved structural elements, in both coding and non-coding regions, that are important for viral replication. Some of these elements are known or predicted to modulate key life cycle events, such as translation and genome replication, involving conformational changes induced by long-range RNA-RNA interactions. One such element is SLVI, a stem-loop (SL) structure located towards the 5' end of the core protein-coding region. This element is predicted to form an alternative RNA-RNA interaction with complementary sequences in the 5'UTR that are themselves involved in the binding of the cellular microRNA 122 (miR122). The switch between 'open' and 'closed' structures involving SLVI has previously been suggested to modulate translation, with lower translation efficiency associated with the 'closed' conformation. In the current study, we have used selective 2'-hydroxyl acylation analysed by primer extension (SHAPE) to validate this RNA-RNA interaction in the absence and presence of miR122. Using site-directed mutations introduced to promote one or other conformation we have found no correlation between the predicted structural conformation and translation enhancement. In addition, we observed no influence on replication compared to wild type, indicating that favouring 'open' or 'closed' interactions also does not unduly alter virus replication. Overall, our data suggests that while SLVI may undergo structural re-arrangements involving a switch from 'open' to 'closed' conformations this has limited phenotypic effect.

Introduction

Hepatitis C virus (HCV) belongs to the genus *Hepacivirus* in the family *Flaviviridae* and, despite the recent development of novel and effective therapies (Gao et al. 2010; Lawitz et al. 2013; Welzel et al. 2017), infects approximately 185 million people globally, causing significant levels of chronic liver disease and hepatocellular carcinoma (Mohd Hanafiah et al. 2013). Like

other flaviviruses HCV possesses a single-stranded, positive(mRNA)-sense genome packaged into an enveloped virus particle (Chambers et al. 1990). The virus genome expresses a single extensive open reading frame (ORF), flanked by highly structured 5' and 3' untranslated regions (UTRs) which, upon delivery to the cytoplasm, is translated to yield a single polyprotein. The latter is co- and post-translationally processed to generate the proteins required for genome replication and particle formation. Thereafter, in a relatively poorly-understood process the genome must act as the template for both translation of the polyprotein and replication resulting in new progeny genomes and, eventually, virus particles. The two processes of translation and replication, unless temporally separated or compartmentalised, must be mutually exclusive and are therefore likely to be controlled.

The limited coding capacity of small RNA viruses necessitates the genome being multi-functional, with control of key events in the replication cycle being influenced by the presence of RNA secondary structures involved in either RNA-RNA interactions and/or the recruitment of viral or host factors (reviewed in (Li & Nagy 2011; Nicholson & White 2014)). Known or predicted conformational changes induced by long-range RNA-RNA interactions in the HCV genome have been described as molecular switches, potentially modulating translation by facilitating the switch from protein synthesis to genome replication (Romero-López et al. 2014; Shetty et al. 2013; Tuplin et al. 2012). The identification of the structures that form the core of these ‘switches’, and the dissection of the underlying molecular mechanism by which they work provides important insights into the replication of HCV and, by extrapolation, related viruses.

The HCV 5'UTR contains RNA signals essential for translation and replication and is an extensively structured region containing four stem-loop domains (SLI-IV; RNA structure naming conventions are detailed in Materials and Methods). Domains SLII-IV of the 5'UTR, along with the first 12-30 nucleotides of the core protein coding sequence, form the internal ribosome entry site (IRES) involved in cap-independent initiation of viral translation (Friebe et al. 2001; Reynolds et al. 1995). Two additional structures within the core coding region, SLV and SLVI, have also been implicated as important RNA elements in viral replication (McMullan et al. 2007). SLVI is a short stem-loop consisting of 54 paired bases, two sub-terminal bulge loops and a terminal loop of 6 nucleotides (Tuplin et al. 2004). In addition to forming functional RNA structures, the 5'UTR provides a platform for recruitment of the liver-specific microRNA 122 (miR122). In contrast to the typically repressive roles of cellular miRNAs, binding of miR122 to

two seed sites (S1 and S2) near the 5' end of the 5'UTR is critical for replication of HCV (Jangra et al. 2010; Jopling et al. 2008; Jopling et al. 2005), as well as stabilising the genome and providing protection against degradation (Li et al. 2013; Sedano & Sarnow 2014; Shimakami et al. 2012).

Intriguingly, a sequence spanning the miR122 seed sites has also been predicted to anneal to complementary sequences that form the basal stem of SLVI. Several indirect methodologies, including RNase cleavage assays and atomic force microscopy, have been used to predict conformational changes in RNA structure involving these sequences (Beguiristain et al. 2005; Díaz-Toledano et al. 2009; García-Sacristán et al. 2015; Kim et al. 2003). Consequently, the conformational changes induced via the 3-way interplay of miR122, the 5'UTR and SLVI may function as a molecular switch, regulating translation and replication. In the simplest scenario, two mutually-exclusive, higher-order RNA structures are predicted as possible; 'open', in which miR122 is bound to the 5'UTR, and the 'closed' structure, in which there is a long-range association (LRA), between the miR122-binding site in the 5'UTR and the base of SLVI in the core-coding region (Fig. 1A).

In this study we have utilised a panel of defined 5'UTR and SLVI mutations to investigate a translation-modulating role for the switch from the 'closed' to the 'open' conformation of this potential molecular switch. SHAPE (selective 2'-hydroxyl acylation analysed by primer extension; (Merino et al. 2005)) analysis confirms previous reports that the change from the 'closed' to the 'open' conformation is influenced by the availability of miR122 (Díaz-Toledano et al. 2009). We further show that the 'closed' confirmation is only achieved in the absence of miR122, or when both miR122 binding is blocked and base pairing within the basal stem of SLVI is prevented. Importantly, we were unable to correlate the 'open' or 'closed' conformations with specific translation phenotypes in either the presence or absence of miR122, and replication of the virus genome was apparently unaffected by these gross structural changes. Therefore, whilst the presence of SLVI is undoubtedly important for regulation of translation, the proposed LRA between the miR122 binding sites in the 5'UTR and the base of SLVI, necessary for the formation of the 'closed' conformation, may not have an important regulatory role in either HCV replication or translation.

Materials and Methods

125

126 **Cell culture and transfection**

127 Huh 7.5 human hepatocellular carcinoma cells were maintained at 37°C, 5% CO_2, in
128 Dulbecco's modified minimal essential medium (DMEM) (Sigma Aldrich) supplemented with
129 10% (v/v) heat-inactivated foetal bovine serum (FBS), 1% non-essential amino acids and
130 2mM L-glutamine (GIBCO, Life Technologies; DMEM-FBS). HeLa cells were maintained at
131 37°C, 5% CO_2, in DMEM supplemented with 10% (v/v) FBS. Cells were seeded in 24-well
132 plates at $1x10^5$ cells/well for translation assays, or $0.8x10^5$ cells/well for replicon assays, in
133 DMEM-FBS 18h prior to transfection.

134 Transfections were carried out with 500ng RNA and 2µl of Lipofectamine 2000 (Life
135 Technologies) as per manufacturers' instructions. In addition, for translation assays 5ng of a
136 capped and polyadenylated Renilla luciferase RNA was added as a transfection control.
137 Transfection media was replaced at 4h with fresh DMEM-FBS. Cell lysates were harvested for
138 analysis at 4h (translation assay) or 4, 21, 28, and 45h (replicon assay). Briefly, cells were
139 washed twice with PBS and lysed with 0.1ml/well Glo Lysis buffer (Promega) for 15 min with
140 shaking. Luciferase readings were determined with Dual-Luciferase (translation assays), or
141 Luciferase (replicon assays), Assay System Kits (Promega) as per manufacturers' instruction.

142

143 **HCV cDNA plasmids, JFH-1 replicon construction and mutagenesis**

144 A variety of numbering or naming schemes have been used to specify RNA stem-loop
145 structures in the HCV genome. Although the most logically extendable scheme involves
146 numbering structures according to the location of the 5' nucleotide within the relevant genome
147 region in an H77 reference sequence (Kuiken et al. 2006), for consistency with previous work on
148 the HCV IRES and long-range structures between coding and non-coding regions, we use the
149 SLI-VI scheme here. For comparison, SLVI is SL87 according to the Kuiken *et al*.
150 nomenclature, due to the 5' most nucleotide being located at nt 87 of the core coding region.

151 A JFH-1 based translation-only reporter construct containing an extended core sequence
152 (CE), to include SLV and VI – designated pJFH1-CEtrans – was generated via modification of
153 pJFH1-luc-trans:ΔNS5B described previously (Tuplin et al. 2015). Overlap PCR was used to
154 generate a DNA consisting of the 5' end of JFH-1, including the first 174nt of JFH-1 core, fused

to the 5' end of Firefly luciferase. An *Age*I/*Xba*I fragment was ligated into similarly digested pJFH1-luc-trans:ΔNS5B to generate pJFH1-CEtrans.

Mutations at miR122 seed site 1 (S1) or/and SLVI were introduced into pJFH1-CEtrans using the QuikChange II site-directed mutagenesis kit as per manufacturers' instructions (Agilent). To disrupt miR122 binding, point mutations $U_{25}A$ and $G_{28}C$ were introduced into the miR122 S1 site to generate pJFH1-CEtrans-S1 (F:5'-GGCGACACACCCCCATGAATCACTC-3' and R:5'-GAGTGATTCATGGGGGTGTGTCGCC-3'). To disrupt the SLVI structure point mutations $C_{436}G$ and $A_{439}U$ (F:5'-CCAGATCGTTGGGGGTATACTTGTTGC-3' and R:5'-GCAACAAGTATACACCCCCAACGATCTGG-3'), and/or $U_{496}A$ and $G_{499}C$ (F:5'-CGACAAGGAAAACATCCGAGCGGTCCCAGC-3' and R:5'-GCTGGGACCGCTCGGATGTTTTCCTTGTCG-3'), were introduced into the 5' and/or 3' stem of SLVI to generate pJFH1-CEtrans-L, pJFH1-CEtrans-R and pJFH1-CEtrans-L/R respectively. Mutants pJFH1-CEtrans-S1/L, pJFH1-CEtrans-S1/R and pJFH1-CEtrans-S1/L/R, containing both the miR122 S1 and SLVI mutations were generated by site-directed mutagenesis of pJFH1-CEtrans-L, pJFH1-CEtrans-R and pJFH1-CEtrans-L/R with the pJFH1-CEtrans-S1 primers described above. All mutations were confirmed by sequence analysis.

A JFH-1 replicon, containing the extended core sequence as above, and designated pJFH1-CErep, was designed based on Con1b-luc-rep (Tuplin et al. 2015). Overlap PCR was used to replace the Con1b 5'UTR with that of JFH-1 within Con1b-rep-luc to generate pJFH1-5'UTR-Con1b-rep. A second overlap PCR generated a DNA containing the 3' end of Firefly luciferase, the EMCV IRES and an ATG codon for NS3, and introduced into the previously described pJ6/JFH-1 (Lindenbach et al. 2005) to generate pJFH1-EMCV. An *Sbf*I/*Not*I fragment from pJFH1-5'UTR-Con1b-rep containing the JFH-1 5'UTR, poliovirus IRES and Firefly luciferase, was inserted into similarly digested pJFH1-EMCV to generate pJFH1-rep. An *Sbf*I/*Pme*I fragment of pJFH-1-CEtrans was inserted into similarly digested pJFH1-rep to generate the core-extended JFH-1 replicon, pJFH1-CErep. Mutations at miR122 S1 and/or SLVI were introduced through *Sbf*I/*Pme*I digestion of the appropriate pJFH1-CEtrans plasmid, and ligation into pJFH1-CErep. This resulted in replicon constructs pJFH1-CErep-S1, pJFH1-CErep-L, pJFH1-CErep-R, pJFH1-CErep-L/R, pJFH1-CErep-S1/L, pJFH1-CErep-S1/R and pJFH1-CErep-S1/L/R.

miR122 duplexing and electrophoretic mobility shift assay

Native (miR122), complementary (miR122-Comp) and S1 mutant (S1-miR122) miR122 RNAs (5'-UGGAGUGUGACAAUGGUGUUUGU-3', 5'-AAACGCCAUUAUCACACUAAAUA-3' and 5'-GGGUGUGUGACAAUGGUGUUUGU-3') were synthesized by Integrated DNA Technologies along with an RNA oligonucleotide corresponding to nucleotides 1-50 of the JFH-1 strain of HCV ($JFH1^{1-50}$).

For addition of miR122 to replicon assays, miR122 RNA (10mM) was duplexed with miR122-Comp (10mM) in a final concentration of 100mM HEPES, 5mM $MgCl_2$, heated at 65°C for 5 min and cooled slowly to room temperature.

For electrophoretic mobility shift assays (EMSA) $JFH1^{1-50}$ RNA (10pmol) was heated for 5 min at 65°C followed by cooling to 35°C for 1 min in a 5µl volume containing 100mM HEPES (pH 7.6), 100mM KCl and 5mM $MgCl_2$. miR122 RNAs were added at molar ratios of 0, 0.5, 1, 1.5, 2, 3 and 5 and incubated for a further 30 min at 37°C. An equal volume of loading dye (30% glycerol, 0.5× TBE and 5mM $MgCl_2$) was added and RNA complexes separated by non-denaturing gel electrophoresis (15% 29:1 acrylamide:bisacrylamide, 0.5× TBE, and 5mM $MgCl_2$) at 150V, 4°C, 3h using a BioRad MiniProtean III gel system. Gels were stained with SYBR Gold (Life Technologies) and RNA visualized using a Typhoon FLA 9500 (GE Healthcare).

***In vitro* RNA transcription**

RNA transcripts were synthesized using a HiScribe™ T7 High Yield RNA Synthesis Kit (NEB), as per manufacturers' instructions, with 1µg of DNA template linearized with *Bsp*HI (for translation templates) or terminated with a 3' *cis*-acting ribozyme from an *Mlu*I linearized template (for replicon templates). Newly transcribed RNA was column-purified using a GeneJET RNA Purification Kit (ThermoFisher Scientific).

RNA modification for SHAPE

10pmol of translation construct-derived RNA transcripts were prepared in 10µl of 0.5× Tris-EDTA (pH8.0) (TE), denatured at 95°C for 3 min and incubated on ice for 3 min prior to addition of 6µl of either a 5mM or 10mM $MgCl_2$ folding buffer [333 mM HEPES (pH8.0), 333mM NaCl and, 16.5mM or 33mM $MgCl_2$]. Samples were allowed to refold at 37°C for 20

min before being divided in half and incubated with either 1µl of 100mM N-methylisatoic anhydride (NMIA) dissolved in DMSO, or 1µl of DMSO, at 37°C for 45 min. For reactions in the presence of miR122 a 3 molar excess of miR122 was added prior to addition of folding buffer. Modified RNAs were column-purified using a GeneJET RNA Purification Kit (ThermoFisher Scientific) to remove miR122 prior to reverse transcription.

5'-[^{32}P]-primer labelling

A total of 60µM of primer was incubated with 10 units of T4 polynucleotide kinase (NEB), 2µl of supplied 10× buffer and 10µl γ-[^{32}P]-ATP (3.7x10^{6} Bq; Perkin Elmer) at 37°C for 30 min followed by heat inactivation at 65°C for 20 min. Radiolabelled primers were purified by separation on Sephadex G-25 Quick Spin Oligo Columns (Roche).

Primer extension for SHAPE

NMIA- or DMSO-treated RNA in 0.5× TE (10µl) was mixed with 3µl of radiolabelled primer, denatured at 95°C for 5 min, annealed at 35°C for 5 min and chilled on ice for 2 min. Reverse transcription (RT) mix (6µl) was added (5× First Strand Buffer, 5 mM DTT, 0.5mM dNTPs; Life Technologies) and samples incubated at 55°C for 1 min prior to addition of 1µl of SuperScript®III (Life Technologies) and further incubation at 55°C for 30 min. The RNA template was degraded by addition of 1µl of 4M NaOH and incubation at 95°C for 5 min before addition of 29µl of acid stop mix (140mM un-buffered Tris-HCl, 73% formamide, 0.43× TBE, 43mM EDTA [pH 8.0], bromophenol blue and xylene cyanol dyes) and further incubation at 95°C for 5 min. Dideoxynucleotide (ddNTP) sequencing markers were generated by the extension of unmodified RNA with addition of 2µl of 20mM ddNTP (TriLink BioTechnologies) prior to addition of RT mix. The cDNA extension products were separated by denaturing electrophoresis [7% (19:1) acrylamide:bisacrylamide, 1× TBE, 7M urea] at 70W for 3-5h depending on product sizes to be analysed. Gels were visualised with a phosphorimager (Typhoon FLA 9500) and densitometry analysis carried out with ImageQuant TL 8.1 software (GE Healthcare Life Sciences). Normalised reactivities indicating exposure of nucleotides in predicted RNA structures were calculated as described previously (Tuplin et al. 2012).

Results

Mutagenesis of a miR122 binding site and the sequences implicated in the LRA

The proposed 'open' and 'closed' structural conformations are determined by complementarity between the 5' nucleotides forming the miR122 binding site and the base of SLVI in the core protein-coding region, together with the presence of exogenous miR122 (Kim et al. 2003). The latter, by binding to the 5'UTR sequences, inhibits the LRA and 'opens' the structure (Fig. 1A). This transition from a 'closed' to an 'open' structure can be predicted bioinformatically using mfold (Zuker 2003) and bifold RNA secondary structure prediction software (Reuter & Mathews 2010), to demonstrate that if the S1 site is occupied by miR122 the 'open' conformation with bound miR122 is energetically more favourable (Fig. S1). To investigate the existence and potential functions of the alternative conformations we first modified our existing JFH-1 translation reporter vector, JFH1-luc-trans:ΔNS5B, to generate a core-extended (CE) version, JFH1-CEtrans, which encompasses the first 174 nucleotides of the core-coding region, thus incorporating SLVI. A JFH-1 based sub-genomic replicon, designated JFH1-CErep, was additionally constructed to include the same core-extended sequence (Fig. 1B). For both JFH1-CEtrans and JFH1-CErep we subsequently undertook a systematic mutagenesis of either, or both, of the complementary sequences required for formation of the LRA.

First, using mfold structure prediction (Zuker 2003), we identified two sites within SLVI at which synonymous substitutions could be introduced that should disrupt formation of the structure (Fig. 1A). Substitutions $C_{436}G$ and $A_{439}U$ in the 5' stem of SLVI (designated 'L' mutants) and $U_{496}A$ and $G_{499}C$ in the 3' stem of SLVI (designated 'R' mutants) independently prevented base pairing of the basal stem of SLVI. Both C_{436} and A_{439} are implicated in the formation of the 'closed' structure and consequently, 'L' mutants were predicted to additionally prevent the LRA due to disruption of the complementarity with the miR122 seed site 1 (S1). Conversely, 'R' mutants would free the 5' sequences forming the basal stem of SLVI to contribute solely to formation of the 'closed' structure. However, since formation of the 'closed' structure would also be dependent on the S1 site being unoccupied by miR122, we also introduced substitutions into the latter (at positions $U_{25}A$ and $G_{28}C$) that were predicted to prevent miR122 binding and at the same time would restore complementarity with the 'L' mutations in SLVI (Fig. 1C, Table 1).

To verify that binding of miR122 to S1 was abrogated in the S1 mutants we conducted electrophoretic mobility shift assays (EMSAs) using synthetic miR122 and an RNA oligonucleotide corresponding to the first 50 nucleotides of JFH-1 ($JFH1^{1-50}$). With the addition of miR122 to unmodified $JFH1^{1-50}$ we observed the expected two complexes with reduced mobility, representative of binding of miR122 to both S1 and S2 seed sites. Saturation of both seed sites was achieved upon addition of a 3:1 molar ratio of miR122:$JFH1^{1-50}$ (Fig. 2A), while addition of an antisense miR122 RNA (miR122-Comp) showed no change in mobility (Fig. 2B). In contrast to unmodified $JFH1^{1-50}$, S1-mutated $JFH1^{1-50}$ only formed the faster migrating single complex, even at a 5:1 molar ratio, indicating that miR122 remained bound to S2 alone (Fig. 2C). Restoration of both mobility-shifted complexes was achieved upon addition of a 50-50 mix of unmodified and S1-modified miR122 (S1-miR122), the latter containing mutations complementary to those introduced in S1 mutated $JFH1^{1-50}$ (Fig. 2D). These studies confirmed that substitutions introduced to the S1 site were sufficient to disrupt miR122 binding to the S1 seed site, but that binding to the S2 seed site was unaffected, in agreement with similar mutation analysis of miR122 binding (Mortimer & Doudna 2013).

To investigate the influence on the conformation of the 5' end of the HCV RNA the L, R and S1 mutations predicted to influence the ‘open’ or ‘closed’ conformation were introduced individually, or in combination, into the core-extended translation and replicon reporters, JFH1-CEtrans and JFH1-CErep respectively, and individual templates validated by sequence analysis (Table 1).

The LRA is detected in the absence, but not presence, of miR122

We have previously used SHAPE mapping to demonstrate a long-range interaction between the 3'UTR of the HCV genome and distal sequences located within the polyprotein-coding region (Tuplin et al. 2012). These interactions occurred only *in cis* and were acutely sensitive to point mutations within the complementary regions. We were therefore confident SHAPE analysis could provide useful insights into the study of the LRA. Three regions of the HCV RNA were analysed to provide data on RNA structure: (1) the 5' base stem of SLVI, (2) the 3' base stem of SLVI and, (3) nts 1-80 of the 5'UTR. Unfortunately, the presence of a highly stable stem-loop (SLI; Fig. 1A) immediately 5' to the S1 miR122 binding site acted as a strong

terminator during cDNA synthesis. Consequently, as others have previously found (Pang et al. 2012), the 5' end of the S1 miR122 binding site (nts 1-20) proved difficult to accurately map due to excessive background signal. Scrutiny of the predicted pattern of base pairing between the miR122 binding site and miR122 also shows that they are highly similar to that proposed between the miR122 binding site and the 5' base stem of SLVI. Together, these issues meant that the S1 region was not informative for defining the 'open' or 'closed' conformation. Determination of the 'closed' structure was therefore based primarily on the structure of SLVI. In particular, nucleotides 434-435 (GG), which are predicted to be paired when involved in the LRA but unpaired in formation of the basal stem of SLVI, and the overall paired/unpaired nature of the 3' side of the basal stem of SLVI (nucleotides 494-507), which would be predominantly unpaired upon formation of the 'closed' structure (Fig. 1A, S1). Preliminary experiments showed that SHAPE mapping of the 5' regions of a variety of unmodified templates *e.g.* JFH1-CEtrans, JFH1-CErep, or a full-length *in vitro* transcribed RNA, resulted in the same NMIA reactivity and resulting structural predictions (data not shown). We conclude from this that the LRA interactions are essentially local in nature and are unaffected by distal sequences in the virus genome. All subsequent SHAPE mapping was conducted using JFH1-CEtrans as template.

We first compared the structural conformations of parental JFH1-CEtrans in the absence of miR122 during the RNA folding reaction, or with a 3:1 molar excess of miR122 to saturate binding to S1 and S2, as determined from EMSAs (Fig. 2A). In the presence of miR122 the basal stem of SLVI was predominantly NMIA-unreactive, indicating that the pairing through this region was in agreement with the structure predicted bioinformatically (Fig. 3A). Indeed, the reactivity of nucleotides 427-447 and 487-507 corresponded very well with the predicted structure of this region of SLVI. As additional validation we determined the NMIA-reactivity of SLVI sequences in JFH1-CEtrans in the presence of a locked-nucleic-acid (LNA) probe, J22. LNA J22 binds with high affinity to nts 21-37 of JFH-1 across the miR122 binding sites, allowing for the determination of the SLVI structure independently of the reversible action of miR122 (Fig. 3C). The resulting SHAPE analysis recapitulated the results observed in the presence of miR122, with little or no reactivity of sequences predicted to form the basal stem of SLVI. These results support the predicted structure of SLVI indicating that, in the presence of miR122, the 'open' conformation predominates.

miR122 is present at high levels in hepatic cells in which HCV replicates (Lagos-Quintana et al. 2002). Nevertheless, since there might be compartmentalisation – in replication complexes for example – where miR122 is limited or absent, we went on to investigate the potential formation of the 'closed' structure by SHAPE in the absence of miR122 (Fig. 3B). Under these conditions we observed gross changes to the structure of the basal region of SLVI. The $G_{434}G_{435}$ motif – predicted to be a key interaction with the S1 site – are highly unreactive, indicating that they are base paired. At the same time, the reactivity of the 3' sequences of the basal stem of SLVI increases. There are significant increases in exposure of nt 490-503 indicative of a more extensive opening out of the SLVI structure. We interpret this as the formation of the 'closed' structure in the absence of miR122, despite the inability to measure the reactivity of nucleotides within the S1 site. In contrast to the results of García-Sacristán *et al.* (García-Sacristán et al. 2015) we were unable to demonstrate a magnesium-dependent preference for the formation of the 'closed' structure while in the presence of miR122. We investigated the structure of the basal stem of SLVI in the parental templates at an increased concentration of 10mM $MgCl_2$ and determined that the 'open' conformation predominated, irrespective of the magnesium concentration (data not shown).

Together, these results are in agreement with a previous conclusion by Díaz-Toledano *et al.* obtained via RNase III cleavage assays (Díaz-Toledano et al. 2009), and are highly indicative of an inhibitory role for miR122 in formation of the 'closed' structure.

The LRA is favoured only when both miR122 binding and the SLVI structure are disrupted

Having investigated the pairing of the basal stem of SLVI and the occurrence of the LRA in unmodified templates, we went on to study the influence of mutations introduced to prevent these interactions, or that we had previously shown prevent miR122 binding. All subsequent analyses were carried out in the presence of miR122.

We first analysed those templates predicted to preferentially form the 'open' conformation (Fig. 4). Modification of the S1 site in template JFH1-CEtrans-S1 (Fig. 4A), shown to abrogate miR122 binding (Fig. 2C), resulted in a NMIA-reactivity pattern almost indistinguishable from the unmodified parental template (compare Fig. 3A with Fig. 4A). Since the $U_{25}A$ and $G_{28}C$ changes in the S1 mutant also prevents interaction with SLVI nts A_{439} and

370 C_{436} respectively, this provides further support that this pattern of NMIA reactivity represents the
371 'open' conformation. Three additional modified templates, JFH1-CEtrans-L, JFH1-CEtrans-L/R
372 and JFH1-CEtrans-S1/R, were also predicted to block the LRA by reducing the complementarity
373 between nucleotides in the S1 site and the basal stem of SLVI (Fig. 1C). NMIA-reactivity of
374 these three templates verified the predicted inhibition of the LRA, as evidenced by the high
375 reactivity of the $G_{434}G_{435}$ motif (Fig. 4B, C, D). Interestingly, in comparison to the parental
376 JFH1-CEtrans, all three templates displayed increases in reactivity in other regions, such as nts
377 427-433 (the 5' basal stem) or nts 491-495 (3' basal stem), suggesting that, while preventing the
378 LRA, the introduced mutations may also lead to generation of an altered SLVI structure
379 (compare line graph to black bars in Fig. 4B, C, D). The mfold predictions for the structure of
380 SLVI containing mutations $C_{436}G$ and $A_{439}U$, and $U_{496}A$ and $G_{499}C$, did not suggest formation of
381 such an altered structure (data not shown) and it is not possible to deduce the precise structure
382 from the NMIA-reactivity plots.
383 We next investigated the conformation of templates containing combinations of
384 mutations that were predicted to favour the LRA and the 'closed' conformation: JFH1-CEtrans-
385 R, JFH1-CEtrans-S1/L and JFH1-CEtrans-S1/L/R (Fig. 5). Unexpectedly, both JFH1-CEtrans-R
386 and JFH1-CEtrans-S1/L/R failed to demonstrate the LRA, again as evidenced by the reactivity of
387 the $G_{434}G_{435}$ motif, as well as the overall lack of reactivity in the 3' basal stem of SLVI that
388 would be expected (Fig. 5A, B). As with JFH1-CEtrans-L and JFH1-CEtrans-L/R, we observed
389 an overall increase in reactivity of the 5' basal stem nucleotides suggestive of a similar disruption
390 to the SLVI structure that was not predicted in mfold calculations (compare Fig. 5A and B with
391 Fig. 4B and C). However, these result suggest that despite significant disruption to the known
392 SLVI structure, the 'closed' structure is not the favoured conformation for the RNA template.
393 In contrast to all other modified templates JFH1-CEtrans-S1/L generated a NMIA-
394 reactivity plot matching that of parental JFH1-CEtrans in the absence of miR122, and is highly
395 indicative of the formation of the 'closed' structure (Fig. 5C). In comparison to a template in
396 which the 'closed' structure is blocked, *i.e.* parental JFH1-CEtrans in the presence of miR122,
397 the mean NMIA-reactivities of the JFH1-CEtrans-S1/L $G_{434}G_{435}$ motif were reduced from 0.38
398 and 1.16 to 0.26 and 0.22 respectively, highlighting a substantial change in the base paired state,
399 especially of G_{435}. Similarly, the average reactivity of nts 490-507 in the 3' basal stem was

400 increased from 0.28 to 0.64 demonstrating the overall increase in reactivity expected when the 5'
401 basal stem of SLVI is bound to the miR122 S1 site in the 'closed' conformation.
402 Taken together the SHAPE analyses show that, in the presence of miR122, the 'closed'
403 conformation only exists when both miR122 binding at S1 is blocked, and nucleotide
404 complementarity between S1 and the 5' basal stem of SLVI is restored.
405
406 *Phenotypic Characterisation of LRA-modified templates*
407 Using SHAPE analyses we determined that, in the presence of miR122, the LRA
408 resulting in the 'closed' conformation, is highly unlikely to form. However, if HCV translation
409 and/or replication occur in locations or complexes in which miR122 is absent then the 'closed'
410 structure is the energetically favourable conformation (Fig. 3B), and as such may influence virus
411 translation and replication. We therefore used selected modified templates with demonstrated
412 changes in conformation, to investigate the effects of the LRA on translation and replication.
413 HCV IRES-mediated translation is known to require the first 12-30 nt of the core protein-
414 coding region (Reynolds et al. 1995). However, to study the effects on translation of the LRA
415 required the additional SLV-SLVI sequences included in the core-extended translation reporter
416 described above and utilised in SHAPE analysis (Fig.1B). We initially compared translation
417 from JFH1-luc-trans:ΔNS5B, containing the minimal core sequence, to the core-extended JFH1-
418 CEtrans reporter. In agreement with previous observations (Kim et al. 2003), translation was
419 significantly decreased (~2.5-fold) with the inclusion of the extended core sequence (Fig. 6A).
420 This reduction in translation is proposed to be a result of formation of the LRA (Kim et al. 2003)
421 and that a high proportion of the JFH1-CEtrans RNA templates exist in the 'closed'
422 conformation (Fig. 1A), and hence are unavailable for use by the cellular translation machinery.
423 As we have demonstrated that the LRA occurs only in the absence of miR122 (Fig. 3), this result
424 implies either the exclusion of miR122 from sites of translation or, an alternative role for the
425 sequences encompassing SLV and SLVI domains in regulating translation. If the observed
426 reduction is a result of the LRA, translation levels should be restored by mutations designed to
427 disrupt the LRA, so forcing the 'open' conformation, and repressed again by compensatory
428 substitutions that – although different from the parental template – restore the LRA and the
429 'closed' conformation.

We therefore compared translation from JFH1-CEtrans with selected modified templates that had shown a distinct conformation in SHAPE analysis. We selected JFH1-CEtrans-S1 as a representative of the 'open' conformation due to the SHAPE analysis most closely matching the SLVI structure observed for parental JFH1-CEtrans. For the 'closed' conformation we were limited to the study of JFH1-CEtrans-S1/L, as the only modified template in which the LRA was demonstrated. In addition, we investigated JFH1-CEtrans-L/R and JFH1-CEtrans-S1/L/R, for which the SHAPE reactivities suggested that the 5' and 3' stem mutations did not recapitulate wild type SLVI as expected due to increased reactivity in the 5' basal stem, but neither were they representative of the 'closed' conformation (Fig. 4C, 5B). We transfected Huh 7.5 cells with 500ng of RNA of each template, in parallel, and normalised translation levels to a Renilla luciferase transfection control RNA (Fig. 6B). As predicted for the 'open' conformation and blocking of the LRA, JFH1-CEtrans-S1 showed a small, but significant, increase in translation level compared to both JFH1-CEtrans and JFH1-CEtrans-S1/L ($p<0.05$). In contrast, JFH1-CEtrans-S1/L, shown to preferentially form the 'closed' structure, did not show the predicted reduction in translation and was unchanged from parental JFH1-CEtrans. Similarly, despite small increases and decreases in translation levels of JFH1-CEtrans-L/R and JFH1-CEtrans-S1/L/R respectively, these were not significantly different when compared to the parental template. This suggests that, even though the wild type SLVI structure is not fully restored, with reduced base pairing remaining in the basal 5' stem, this did not impact translation.

The limited changes in phenotype observed strongly suggested that the difference observed between JFH1-luc-trans:ΔNS5B and JFH1-CEtrans is due to an as yet unidentified role for SLV and VI, and is not miR122 or LRA dependent. In the presence of miR122 both these templates exhibit the 'open' conformation as determined by SHAPE analysis (Fig. 3A, 4A). Due to the mutations introduced into JFH1-CEtrans-S1 only JFH1-CEtrans is capable of forming the 'closed' conformation which, in the absence of miR122, is the preferred conformation (Fig. 3B). As the switch between the two conformations is miR122 dependent we reasoned that, if the 'closed' confirmation is in fact responsible for the reduction in translation of JFH1-CEtrans, we would observe a similar difference when comparing JFH1-CEtrans ('closed') to JFH1-CEtrans-S1 ('open') in cells lacking miR122. We therefore investigated translation of JFH1-luc-trans:ΔNS5B, JFH1-CEtrans, JFH1-CEtrans-S1 and JFH1-CEtrans-S1/L in HeLa cells, which are naturally lacking in miR122 (Jopling et al. 2005) (Fig. 6C). Overall we observed translation

levels that were ~10-fold lower in HeLa cells than in Huh 7.5 cells. However, the relative translation phenotypes remained the same, with a significant reduction in translation for JFH1-CEtrans, and all other templates that contained the core-extended sequence. Additionally, no significant changes were observed between JFH1-CEtrans and JFH1-CEtrans-S1, or JFH1-CEtrans-S1/L, which is also expected to form the 'closed' conformation in the absence of miR122. This supports our contention that formation of the LRA does not account for the change in translation phenotype between JFH1-luc-trans:ΔNS5B and JFH1-CEtrans, and conclude that – although the presence of SLVI clearly reduces translation (Fig. 6A, C) – this is unrelated to the LRA and any miR122 induced switch between the 'open' and 'closed' conformations.

With no observable link between translation levels and the conformations demonstrated by SHAPE analysis we went on to investigate whether there were differences in replication between our structurally modified templates. To achieve this we used a core-extended version of a JFH-1 replicon, JFH1-CErep. Huh 7.5 cells were transfected with 500ng of template RNA, containing the same modifications as above, and replication recorded as luciferase activity over a 45h time course. Our results show that for JFH1-CErep-L/R, where mutations were engineered solely within SLVI, replication was not significantly altered from the unmodified parental replicon, in keeping with the results for translation (Fig. 6D, 6B). In contrast, mutants JFH1-CErep-S1, JFH1-CErep-S1/L and JFH1-CErep-S1/L/R, in which miR122 binding to S1 is blocked, all showed a >10-fold, highly significant reduction in the level of replication ($p<0.01$) (Fig. 6D). This is entirely consistent with our current understanding that miR122 binding to the 5'UTR of HCV is important for HCV replication (Jangra et al. 2010; Jopling et al. 2005). The addition of modified S1-miR122 to the RNA transfection mix, to complement the S1 mutations in the replicon, restored replication of JFH1-CErep-S1 to parental levels, demonstrating that the observed reductions in replication are due entirely to disruption of miR122 binding and not a consequence of possible changes in conformation promoted by the LRA (Fig. 6E).

These results demonstrate that, while miR122 binding has a profound effect on the replication of the HCV genome, neither replication nor translation phenotypes are significantly influenced by modifications to SLVI that preferentially form the 'open' or 'closed' conformations of the LRA.

491 Discussion
492
493 How are the competing events of single-stranded, positive-sense, RNA virus translation
494 and replication separated? At least early in the replication cycle, before compartmentalization
495 into membrane-bound replication vesicles, these must involve interaction of the translating
496 ribosome or the viral polymerase with the same template. One strategy, typified by poliovirus,
497 requires the accumulation of one or more viral translation products to initiate genome replication
498 (Barton & Flanegan 1997; Jurgens & Flanegan 2003). In this case, ribonucleoprotein complexes
499 form involving phylogenetically conserved RNA stem-loop structures. Since many positive-
500 sense single-stranded RNA viruses have small genomes, the adoption of higher-order structures
501 – that may vary in conformation depending upon the environment or availability of interacting
502 proteins – effectively increases the level of control that can be exerted during the replication
503 cycle. In particular, structures capable of forming long-range interactions are of interest as they
504 may have the capability to cyclize the genome (Alvarez et al. 2005) or – by adopting alternate
505 conformation – riboswitches (Ooms et al. 2004; Shetty et al. 2013; Wang & White 2007)
506 The HCV genome is extensively structured (Mauger et al. 2015; Simmonds et al. 2004;
507 Tuplin et al. 2012) and a number of long-range interactions have been predicted within it (Fricke
508 et al. 2015), some having demonstrable involvement in important aspects of the HCV replication
509 cycle (Diviney et al. 2008; Romero-López et al. 2014; Romero-López & Berzal-Herranz 2009;
510 Shetty et al. 2013; Tuplin et al. 2015; You & Rice 2008). Of these, the long-range association
511 (LRA) between nts 23-31 encompassing miR122 seed site 1 in the 5'UTR, and complementary
512 nts 433-441 located in the 5' basal stem of SLVI within the core protein coding region
513 (Beguiristain et al. 2005; Díaz-Toledano et al. 2009; García-Sacristán et al. 2015; Kim et al.
514 2003), may adopt ‘open’ and ‘closed’ conformations, and is predicted to modulate the switch
515 between translation and replication of the virus genome (Fig. 1A) (Kim et al. 2003). The ‘open’
516 conformation (*i.e.* no LRA) is proposed to favour translation, whereas the ‘closed’ conformation
517 restricts access of the ribosome to sequences within the coding region implicated in genome
518 translation, thereby favouring replication.
519 To investigate the structure and function of the ‘open’ and ‘closed’ conformations in
520 greater detail we have mapped the native structure using SHAPE in the presence and absence of
521 miR122. We have additionally extensively mutagenised sequences implicated in formation of

both the ‘open’ and ‘closed’ conformations, mapped their structure by SHAPE and investigated the resulting influence on translation and genome replication.

Although the strong stem-loop (SLI) in the 5'UTR confounded SHAPE interrogation of sequences forming the S1 site of miR122 binding, those contributing to the basal stem of SLVI were readily mapped. Having determined the influence on miR122 binding of mutations in the S1 site (Fig. 2) we inferred the LRA and formation of the ‘closed’ structure from exposure or otherwise of the basal stem of SLVI. The LRA was detectable only under very specific conditions, including an *in vitro* assay in which miR122 was omitted. Similarly, mutagenesis of the template within the S1 miR122 binding site (to prevent miR122 binding) and introduction of complementary mutations to the 5' basal stem of SLVI allowed the LRA to be inferred. In contrast, in the presence of miR122, and/or unmodified sequences at the basal stem of SLVI, we were unable to detect the LRA and formation of the ‘closed’ structure. We propose that, under conditions in which miR122 is present in significant amounts, the phylogenetically conserved basal stem of SLVI is unlikely to separate to form a long-range association.

However, incorporation of 5' (L) and 3' (R) mutations to SLVI did lead to structural changes within stem-loop that were not predicted by mfold. With the exception of JFH1-CEtrans-S1/L, which clearly adopts the ‘closed’ conformation, all the tested substitutions to the basal stem of SLVI increased the NMIA-reactivity of the structure (Fig. 4 and 5), indicating a reduction in complementary pairing that was more extensive than the sites of modification. In addition, when not paired with the 5' mutations, the 3' mutants (JFH1-CEtrans-R and JFH1-CEtrans-S1/R) showed further modification of the SLVI structure with the loss of reactivity of nts 500-501 (Fig. 5A and 4D). In these cases, it is clear that SLVI had undergone more extensive alteration of base pairing and structure. Previous studies of SLVI ,independent of LRA disruption, were shown to result in alteration to the translation phenotype (Vassilaki et al. 2008). Without a greater understanding of the RNA structure in this region, for example by expanding the region analysed by SHAPE mapping, we do not think a complete interpretation of the relationship between RNA structure and phenotype is possible.

Notwithstanding the potential for the LRA forming during HCV infection *in vivo*, we went on to analyse HCV translation and replication from templates in which we engineered the ‘open’ or ‘closed’ conformations by mutagenesis of the complementary pairing critical for LRA formation. We reasoned that, if dramatic differences were observable, this might indicate a role

for the LRA and our ability to detect the 'closed' structure *in vitro* might not be representative of conditions *in vivo*. For example, cellular proteins could influence the formation of the LRA or miR122 may be limiting or absent at certain stages of the replication cycle .

We investigated translation from a core-extended template transfected into Huh 7.5 cells. As expected from previous studies (Kim et al. 2003), extension of core-encoding sequences – to encompass SLVI – reduced reporter gene expression by ~50%. When normalised to this lower level of translation, the template engineered to adopt the 'closed' conformation (JFH1-CEtrans-S1/L) exhibited levels of translation essentially indistinguishable from the control. In contrast, the template unable to recruit miR122 to the S1 seed site (JFH1-CEtrans-S1) and therefore solely adopting the 'open' conformation, exhibited a slight but significant increase in translation (Fig. 6B). Compared to its vital role in viral replication, the role of miR122 in stimulating HCV translation is not as clear, with some reports suggesting mutations in miR122 seed sites do not lead to changes in translation (Jopling et al. 2005) and others observing decreases in translation upon mutation of either, or both, seed sites (Jangra et al. 2010). Our results for JFH1-CEtrans-S1 and JFH1-CEtrans-S1/L/R, both adopting an 'open' conformation, would support the studies by Jopling and colleagues (Jopling et al. 2005). Despite inhibition of miR122 binding at the S1 site, both templates were still able to recruit miR122 to the S2 site (Fig. 2), thus maintaining parental, or near-parental levels of translation. Therefore, templates of known conformation with regard to the LRA did not show a correlation between a closed structure and a reduction in translation, and opening the structure only led to a minor increase in translation in one template, JFH1-CEtrans-S1. In addition, relative translation phenotypes in HeLa cells were comparable to Huh 7.5 cells demonstrating that the presence of SLVI is sufficient to account for the reduction in translation observed between JFH1-luc-trans:ΔNS5B and JFH1-CEtrans (Fig. 6B, C). The presence of SLVI has also been shown to influence translation through modulation of RNA interactions involving domain 5BSL3.2 (Ventura et al. 2017). Such interactions may contribute to the translation phenotypes we have demonstrated here to be independent of the LRA.

In contrast to the results obtained using translation templates bearing mutations to destroy/recreate the LRA, analysis of genome replication bearing identical mutations was easier to interpret. In these, any mutation of the S1 miR122 seed site reduced replication by ~2 $\log_{10}$ at 28h post-transfection (Fig. 6C) and this phenotype could be readily and fully rescued by provision of a complementary S1-miR122 *in trans*. These results imply that the structures

adopted by sequences predicted to be involved in the LRA either have no influence on genome replication, or that the influence is negligible when compared to the known impact of reduced miR122 binding (Jopling et al. 2008; Jopling et al. 2005; Li et al. 2013).

Taken together, these studies suggest that the proposed LRA between the S1 binding site and the basal stem of SLVI is unlikely to contribute to temporal control of genome translation and replication. In the absence of introduced complementary mutations we could only demonstrate formation of the LRA-associated 'closed' structure under very specific conditions in which miR122 was absent (Fig. 3B). Whether such conditions occur *in vivo* is unclear. An estimated 66,000 copies of miR122 have been reported in hepatocytes (Jopling 2012) and Luna *et al*., (Luna et al. 2015) have reported that HCV replication de-represses cellular targets of miR122, implying that the replicating virus genome acts as a 'sponge' to sequester miR122. Although the latter suggests that miR122 is limiting, it is unlikely to be early in the infection cycle. At this time a small number of genomes are present and temporal control of genome translation and replication is likely critical outside the compartmentalisation offered by membrane-bound replication complexes (Wölk et al. 2008) (Miyanari et al. 2003).

Conclusions

Conformational changes in RNA structure are one method by which RNA viruses can modulate essential genome functions such as translation and replication. In this study we demonstrate that one such predicted conformational change, the LRA, involving complementary sequences in the HCV IRES and a core gene stem-loop structure, is unlikely to act as a modulator between translation and replication. We have shown that switching between the 'open' and 'closed' conformations is a miR122 dependent process and confirmed that presence of the core stem-loop structure SLVI results in a drop in translation activity. However we have demonstrated that templates preferentially forming either the 'open' or 'closed' conformation are not associated with any translation or replication phenotypes. Instead we propose that the stem-loop structure SLVI, mediates translation via other, as yet undefined mechanisms.

References

615 Alvarez DE, Lodeiro MF, Ludueña SJ, Pietrasanta LI, and Gamarnik AV. 2005. Long-range
616 RNA-RNA interactions circularize the dengue virus genome. *J Virol* 79:6631-6643.
617 79/11/6631 [pii]
618 10.1128/JVI.79.11.6631-6643.2005
619 Barton DJ, and Flanegan JB. 1997. Synchronous replication of poliovirus RNA: initiation of
620 negative-strand RNA synthesis requires the guanidine-inhibited activity of protein
621 2C. *J Virol* 71:8482-8489.
622 Beguiristain N, Robertson HD, and Gómez J. 2005. RNase III cleavage demonstrates a long
623 range RNA: RNA duplex element flanking the hepatitis C virus internal ribosome
624 entry site. *Nucleic Acids Res* 33:5250-5261. 10.1093/nar/gki822
625 Chambers TJ, Hahn CS, Galler R, and Rice CM. 1990. Flavivirus genome organization,
626 expression, and replication. *Annu Rev Microbiol* 44:649-688.
627 10.1146/annurev.mi.44.100190.003245
628 Diviney S, Tuplin A, Struthers M, Armstrong V, Elliott RM, Simmonds P, and Evans DJ. 2008.
629 A hepatitis C virus cis-acting replication element forms a long-range RNA-RNA
630 interaction with upstream RNA sequences in NS5B. *J Virol* 82:9008-9022.
631 10.1128/JVI.02326-07
632 Díaz-Toledano R, Ariza-Mateos A, Birk A, Martínez-García B, and Gómez J. 2009. In vitro
633 characterization of a miR-122-sensitive double-helical switch element in the 5'
634 region of hepatitis C virus RNA. *Nucleic Acids Res* 37:5498-5510. gkp553 [pii]
635 10.1093/nar/gkp553
636 Fricke M, Dünnes N, Zayas M, Bartenschlager R, Niepmann M, and Marz M. 2015. Conserved
637 RNA secondary structures and long-range interactions in hepatitis C viruses. R*NA*
638 *2*1:1219-1232. 10.1261/rna.049338.114
639 Friebe P, Lohmann V, Krieger N, and Bartenschlager R. 2001. Sequences in the 5 '
640 nontranslated region of hepatitis C virus required for RNA replication. J*ournal of*
641 *Virology 7*5:12047-12057.
642 Gao M, Nettles RE, Belema M, Snyder LB, Nguyen VN, Fridell RA, Serrano-Wu MH, Langley
643 DR, Sun JH, O'Boyle DR, Lemm JA, Wang C, Knipe JO, Chien C, Colonno RJ, Grasela
644 DM, Meanwell NA, and Hamann LG. 2010. Chemical genetics strategy identifies an
645 HCV NS5A inhibitor with a potent clinical effect. N*ature 4*65:96-100.
646 10.1038/nature08960
647 García-Sacristán A, Moreno M, Ariza-Mateos A, López-Camacho E, Jáudenes RM, Vázquez L,
648 Gómez J, Martín-Gago J, and Briones C. 2015. A magnesium-induced RNA
649 conformational switch at the internal ribosome entry site of hepatitis C virus
650 genome visualized by atomic force microscopy. N*ucleic Acids Res 4*3:565-580.
651 10.1093/nar/gku1299
652 Jangra RK, Yi M, and Lemon SM. 2010. Regulation of hepatitis C virus translation and
653 infectious virus production by the microRNA miR-122. J *Virol 8*4:6615-6625.
654 JVI.00417-10 [pii]
655 10.1128/JVI.00417-10
656 Jopling C. 2012. Liver-specific microRNA-122: Biogenesis and function. RN*A Biol 9:*137-142.
657 10.4161/rna.18827
658 Jopling CL, Schütz S, and Sarnow P. 2008. Position-dependent function for a tandem
659 microRNA miR-122-binding site located in the hepatitis C virus RNA genome. C*ell*
660 *Host Microbe 4:*77-85. S1931-3128(08)00173-X [pii]

10.1016/j.chom.2008.05.013
Jopling CL, Yi M, Lancaster AM, Lemon SM, and Sarnow P. 2005. Modulation of hepatitis C virus RNA abundance by a liver-specific MicroRNA. Sci*ence 309*:1577-1581. 309/5740/1577 [pii]
10.1126/science.1113329
Jurgens C, and Flanegan JB. 2003. Initiation of poliovirus negative-strand RNA synthesis requires precursor forms of p2 proteins. J Vi*rol 77:1*075-1083.
Kim YK, Lee SH, Kim CS, Seol SK, and Jang SK. 2003. Long-range RNA-RNA interaction between the 5' nontranslated region and the core-coding sequences of hepatitis C virus modulates the IRES-dependent translation. RNA *9:59*9-606.
Kuiken C, Combet C, Bukh J, Shin-I T, Deleage G, Mizokami M, Richardson R, Sablon E, Yusim K, Pawlotsky JM, Simmonds P, and Los Alamos HIVdg. 2006. A comprehensive system for consistent numbering of HCV sequences, proteins and epitopes. Hepa*tology 44:1*355-1361. 10.1002/hep.21377
Lagos-Quintana M, Rauhut R, Yalcin A, Meyer J, Lendeckel W, and Tuschl T. 2002. Identification of tissue-specific microRNAs from mouse. Curr *Biol 12:7*35-739.
Lawitz E, Lalezari JP, Hassanein T, Kowdley KV, Poordad FF, Sheikh AM, Afdhal NH, Bernstein DE, Dejesus E, Freilich B, Nelson DR, Dieterich DT, Jacobson IM, Jensen D, Abrams GA, Darling JM, Rodriguez-Torres M, Reddy KR, Sulkowski MS, Bzowej NH, Hyland RH, Mo H, Lin M, Mader M, Hindes R, Albanis E, Symonds WT, Berrey MM, and Muir A. 2013. Sofosbuvir in combination with peginterferon alfa-2a and ribavirin for non-cirrhotic, treatment-naive patients with genotypes 1, 2, and 3 hepatitis C infection: a randomised, double-blind, phase 2 trial. Lanc*et Infect Dis 13:4*01-408. 10.1016/S1473-3099(13)70033-1
Li Y, Masaki T, Yamane D, McGivern DR, and Lemon SM. 2013. Competing and noncompeting activities of miR-122 and the 5' exonuclease Xrn1 in regulation of hepatitis C virus replication. Proc *Natl Acad Sci U S A 110:*1881-1886. 10.1073/pnas.1213515110
Li Z, and Nagy PD. 2011. Diverse roles of host RNA binding proteins in RNA virus replication. RNA *Biol 8:30*5-315.
Lindenbach BD, Evans MJ, Syder AJ, Wolk B, Tellinghuisen TL, Liu CC, Maruyama T, Hynes RO, Burton DR, McKeating JA, and Rice CM. 2005. Complete replication of hepatitis C virus in cell culture. Sci*ence 309:*623-626.
Luna JM, Scheel TK, Danino T, Shaw KS, Mele A, Fak JJ, Nishiuchi E, Takacs CN, Catanese MT, de Jong YP, Jacobson IM, Rice CM, and Darnell RB. 2015. Hepatitis C virus RNA functionally sequesters miR-122. Cell *160:*1099-1110. 10.1016/j.cell.2015.02.025
Mauger DM, Golden M, Yamane D, Williford S, Lemon SM, Martin DP, and Weeks KM. 2015. Functionally conserved architecture of hepatitis C virus RNA genomes. Proc *Natl Acad Sci U S A 112:*3692-3697. 10.1073/pnas.1416266112
McMullan LK, Grakoui A, Evans MJ, Mihalik K, Puig M, Branch AD, Feinstone SM, and Rice CM. 2007. Evidence for a functional RNA element in the hepatitis C virus core gene. Proc *Natl Acad Sci U S A 104:*2879-2884. 0611267104 [pii]
10.1073/pnas.0611267104
Merino EJ, Wilkinson KA, Coughlan JL, and Weeks KM. 2005. RNA structure analysis at single nucleotide resolution by selective 2'-hydroxyl acylation and primer extension (SHAPE). J Am *Chem Soc 127:4*223-4231. 10.1021/ja043822v

Miyanari Y, Hijikata M, Yamaji M, Hosaka M, Takahashi H, and Shimotohno K. 2003. Hepatitis C virus non-structural proteins in the probable membranous compartment function in viral genome replication. J Bio*l Chem 278:5*0301-50308. 10.1074/jbc.M305684200

Mohd Hanafiah K, Groeger J, Flaxman AD, and Wiersma ST. 2013. Global epidemiology of hepatitis C virus infection: new estimates of age-specific antibody to HCV seroprevalence. Hepat*ology 57:13*33-1342. 10.1002/hep.26141

Mortimer SA, and Doudna JA. 2013. Unconventional miR-122 binding stabilizes the HCV genome by forming a trimolecular RNA structure. Nucle*ic Acids Res 41:42*30-4240. 10.1093/nar/gkt075

Nicholson BL, and White KA. 2014. Functional long-range RNA-RNA interactions in positive-strand RNA viruses. Nat R*ev Microbiol 12:49*3-504. 10.1038/nrmicro3288

Ooms M, Huthoff H, Russell R, Liang C, and Berkhout B. 2004. A riboswitch regulates RNA dimerization and packaging in human immunodeficiency virus type 1 virions. J Vir*ol 78:10*814-10819. 10.1128/JVI.78.19.10814-10819.2004

Pang PS, Pham EA, Elazar M, Patel SG, Eckart MR, and Glenn JS. 2012. Structural map of a microRNA-122: hepatitis C virus complex. J Vir*ol 86:12*50-1254. JVI.06367-11 [pii] 10.1128/JVI.06367-11

Reuter JS, and Mathews DH. 2010. RNAstructure: software for RNA secondary structure prediction and analysis. BMC Bi*oinformatics 11:129*. 10.1186/1471-2105-11-129

Reynolds JE, Kaminski A, Kettinen HJ, Grace K, Clarke BE, Carroll AR, Rowlands DJ, and Jackson RJ. 1995. Unique features of internal initiation of hepatitis C virus RNA translation. EMBO J *14:601*0-6020.

Romero-López C, Barroso-Deljesus A, García-Sacristán A, Briones C, and Berzal-Herranz A. 2014. End-to-end crosstalk within the hepatitis C virus genome mediates the conformational switch of the 3'X-tail region. Nucle*ic Acids Res 42:567*-582. 10.1093/nar/gkt841

Romero-López C, and Berzal-Herranz A. 2009. A long-range RNA-RNA interaction between the 5' and 3' ends of the HCV genome. RNA 15*:174*0-1752. rna.1680809 [pii] 10.1261/rna.1680809

Sedano CD, and Sarnow P. 2014. Hepatitis C virus subverts liver-specific miR-122 to protect the viral genome from exoribonuclease Xrn2. Cell Ho*st Microbe 16:257*-264. 10.1016/j.chom.2014.07.006

Shetty S, Stefanovic S, and Mihailescu MR. 2013. Hepatitis C virus RNA: molecular switches mediated by long-range RNA-RNA interactions? Nucleic *Acids Res 41:2526*-2540. 10.1093/nar/gks1318

Shimakami T, Yamane D, Jangra RK, Kempf BJ, Spaniel C, Barton DJ, and Lemon SM. 2012. Stabilization of hepatitis C virus RNA by an Ago2-miR-122 complex. Proc Na*tl Acad Sci U S A 109:941*-946. 10.1073/pnas.1112263109

Simmonds P, Tuplin A, and Evans DJ. 2004. Detection of genome-scale ordered RNA structure (GORS) in genomes of positive-stranded RNA viruses: Implications for virus evolution and host persistence. RNA 10:*1337*-1351. 10.1261/rna.7640104

Tuplin A, Evans DJ, and Simmonds P. 2004. Detailed mapping of RNA secondary structures in core and NS5B-encoding region sequences of hepatitis C virus by RNase cleavage and novel bioinformatic prediction methods. J Gen V*irol 85:3037*-3047. 10.1099/vir.0.80141-0

753 Tuplin A, Struthers M, Cook J, Bentley K, and Evans DJ. 2015. Inhibition of HCV translation
754 by disrupting the structure and interactions of the viral CRE and 3' X-tail. Nucleic
755 *Acids Res 43:2914*-2926. 10.1093/nar/gkv142
756 Tuplin A, Struthers M, Simmonds P, and Evans DJ. 2012. A twist in the tail: SHAPE mapping
757 of long-range interactions and structural rearrangements of RNA elements involved
758 in HCV replication. Nucleic *Acids Res 40:6908*-6921. 10.1093/nar/gks370
759 Vassilaki N, Friebe P, Meuleman P, Kallis S, Kaul A, Paranhos-Baccalà G, Leroux-Roels G,
760 Mavromara P, and Bartenschlager R. 2008. Role of the hepatitis C virus core+1 open
761 reading frame and core cis-acting RNA elements in viral RNA translation and
762 replication. J Virol *82:1150*3-11515. JVI.01640-08 [pii]
763 10.1128/JVI.01640-08
764 Ventura M, Martin L, Jaubert C, Andréola ML, and Masante C. 2017. Hepatitis C virus
765 intragenomic interactions are modulated by the SLVI RNA structure of the core
766 coding sequence. J Gen Vi*rol 98:633*-642. 10.1099/jgv.0.000719
767 Wang S, and White KA. 2007. Riboswitching on RNA virus replication. Proc Nat*l Acad Sci U S*
768 *A 104:10406*-10411. 10.1073/pnas.0704178104
769 Welzel TM, Nelson DR, Morelli G, Di Bisceglie A, Reddy RK, Kuo A, Lim JK, Darling J, Pockros
770 P, Galati JS, Frazier LM, Alqahtani S, Sulkowski MS, Vainorius M, Akushevich L, Fried
771 MW, Zeuzem S, and Group H-TS. 2017. Effectiveness and safety of sofosbuvir plus
772 ribavirin for the treatment of HCV genotype 2 infection: results of the real-world,
773 clinical practice HCV-TARGET study. Gut 66:1*844*-1852. 10.1136/gutjnl-2016-
774 311609
775 Wölk B, Büchele B, Moradpour D, and Rice CM. 2008. A dynamic view of hepatitis C virus
776 replication complexes. J Virol *82:10519*-10531. 10.1128/JVI.00640-08
777 You S, and Rice CM. 2008. 3' RNA elements in hepatitis C virus replication: kissing partners
778 and long poly(U). J Virol *82:184-1*95.
779 Zuker M. 2003. Mfold web server for nucleic acid folding and hybridization prediction.
780 Nucleic *Acids Res 31:3406*-3415.
781
782
783
784

Figure 1(on next page)

Schematics of RNA structures and templates used.

(A) The predicted ‘open’ and ‘closed’ conformations of the HCV 5'UTR from SL I-VI with the addition, or loss, of miR122 as shown. S1 and S2 highlight the known binding sites of miR122. Black arrows indicate position and directionality of SHAPE primers. The red box shows expanded view of nucleotides 1-42 of JFH-1 with miR122 (lower case) bound to sites S1 and S2, with the blue box showing expanded view of nucleotides 428-507 of JFH-1 encompassing SLVI . Nucleotides in red are those predicted to be directly involved in formation of the LRA and mutations are indicated by feint black arrows indicating the substitutions made. Figure recreated and adapted from (Díaz-Toledano et al. 2009) . (B) The core-extended JFH-1 bicistronic translation reporter (top) and replicon (bottom). (C) The miR122 binding sites and SLVI with 5' stem (L), 3' stem (R) and S1 mutations displayed. The predicted blocking of miR122 binding, or SLVI formation, of each pair of mutations is shown. Black arrows represent the relative likely conformation, ‘open’ or ‘closed’, predicted to be favoured by each template.

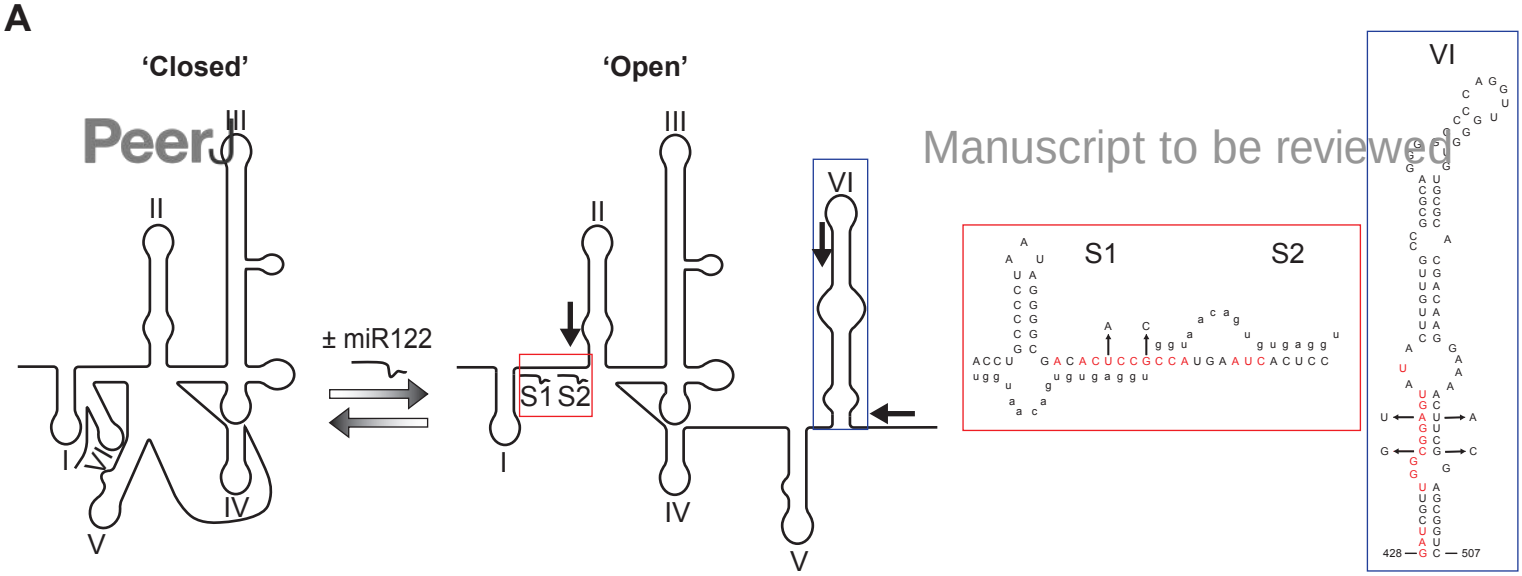

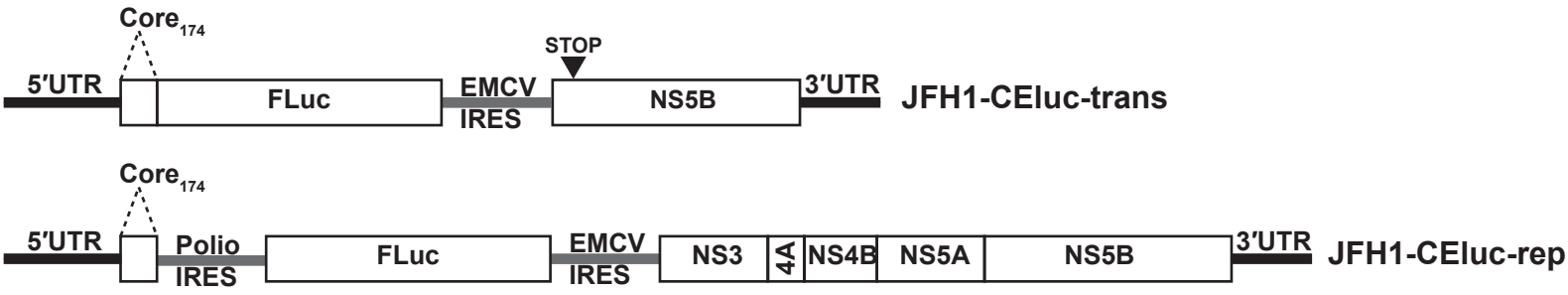

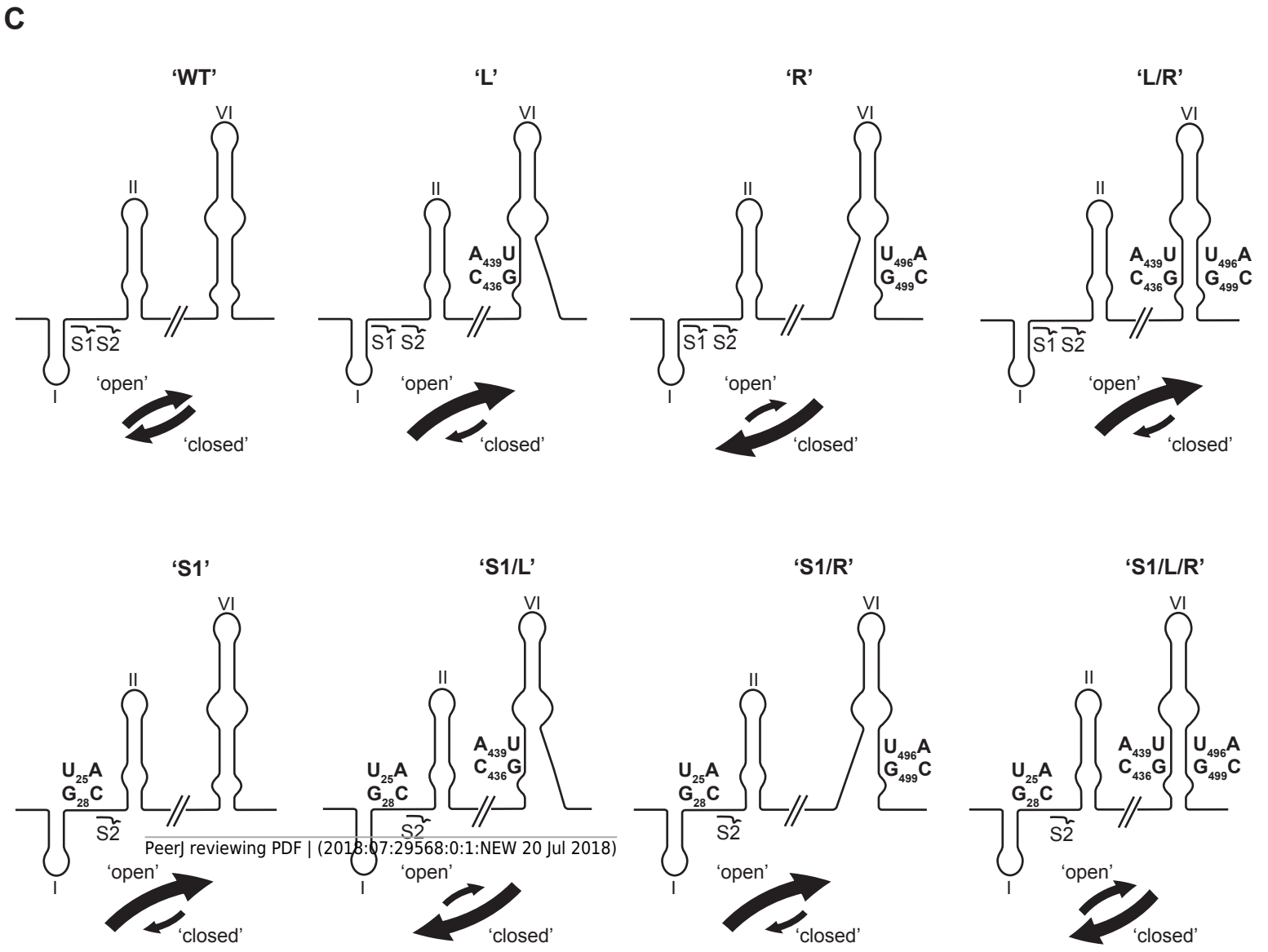

Figure 2(on next page)

RNA-RNA electrophoretic mobility gel shift assays of miR122 binding to JFH-1 5'UTR.

A synthetic RNA of nts 1-50 of JFH-1 ($JFH1^{1-50}$) was complexed with increasing molar ratios of (A) wild type or (B) antisense synthetic miR122 and separated by non-denaturing PAGE. $JFH1^{1-50}$ mutated at the S1 binding site was similarly complexed with (C) wild type or (D) wild type plus an S1-mutated miR122 and separated by non-denaturing PAGE. miR122 binding was denoted by 1 (+ miR122) or 2 (++ miR122) reductions in RNA mobility compared to $JFH1^{1-50}$ control with no miR122 present (lane 1, A-D).

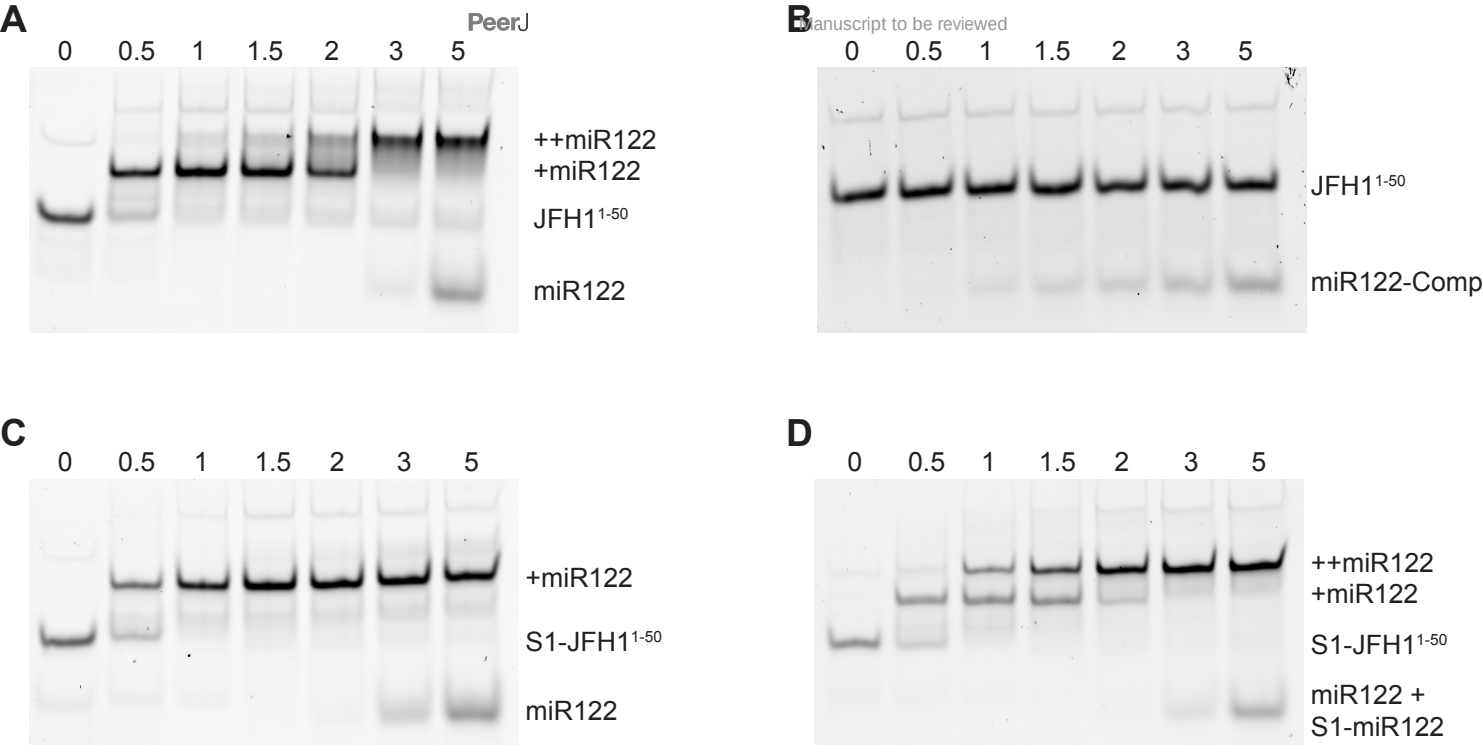

Figure 3(on next page)

SHAPE analysis of parental template plus/minus miR122.

SHAPE reactivities are shown for (A) JFH1-CEtrans plus miR122, (B) JFH1-CEtrans minus miR122, and (C) JFH1-CEtrans plus LNA J22, with predicted (P) and observed (O) conformations given top right below template name. Black bars show normalised SHAPE reactivities of nucleotides 427-447 and 487-507, encompassing the 5' and 3' basal stems of SLVI respectively. Nucleotides with a reactivity of <0.4 are considered unreactive and therefore base-paired. Shaded regions highlight nucleotides of importance in determining 'open' or 'closed' conformations: specifically the 5' $G_{434}G_{435}$ motif and 3' nucleotides 494-507. The superimposed red line indicates the exposure of JFH1-CEtrans plus miR122, and is included on all plots for comparison of reactivities between a demonstrated 'open' conformation and the observed reactivity of additional templates. A maximum negative reactivity was set at -0.1. Unless otherwise stated, error bars represent the SD of a minimum of 2 independent gel analyses for 2 replicate RNA-NMIA folding reactions. Figure 3c was derived from only one replicate folding reaction.

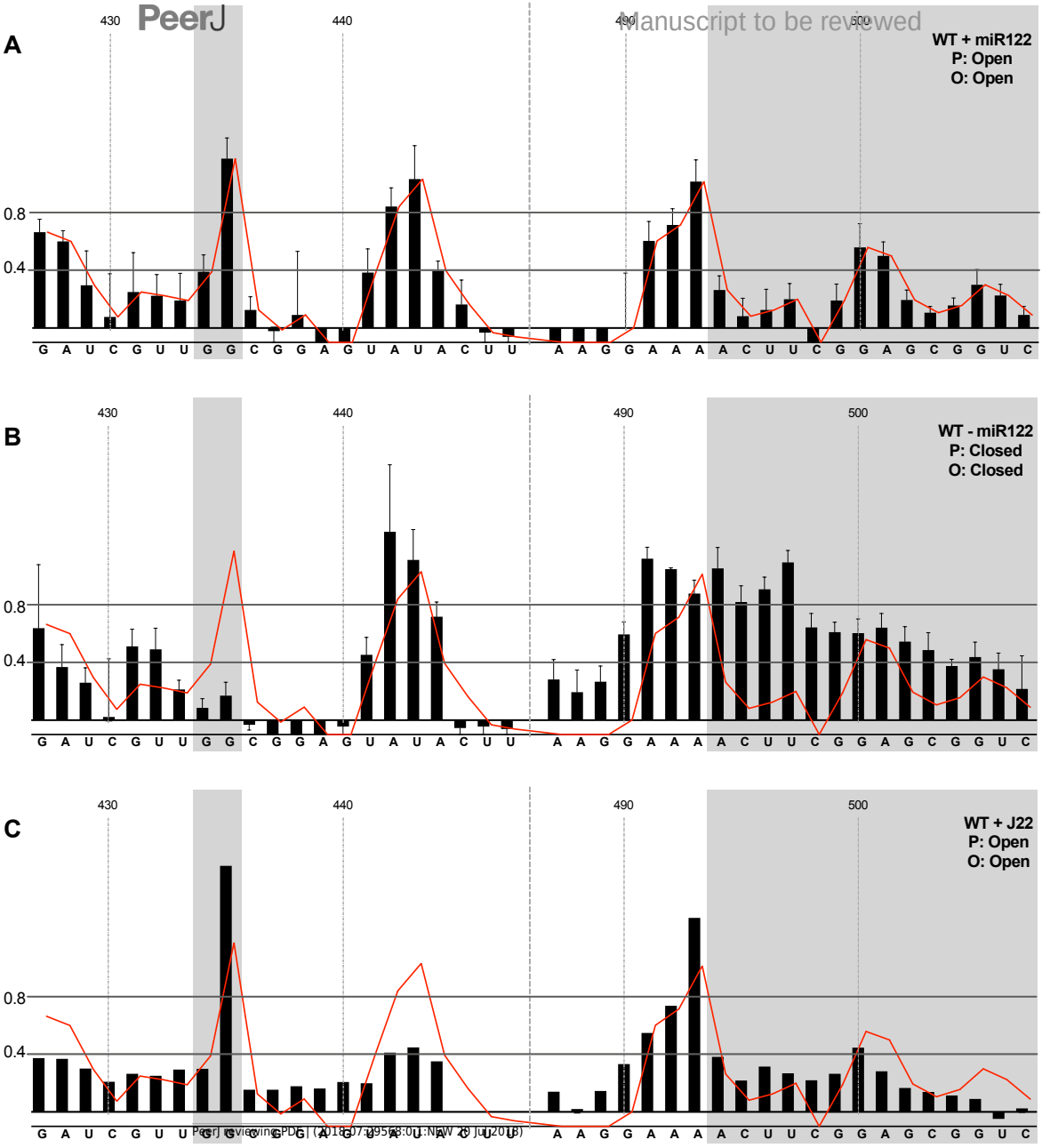

Figure 4(on next page)

SHAPE analysis of S1 and SLVI mutants with predicted ‘open’ conformation.

SHAPE reactivities are shown for (A) JFH1-CEtrans-S1, (B) JFH1-CEtrans-L, (C) JFH1-CEtrans-L/R, and (D) JFH1-CEtrans-S1/R, with predicted (P) and observed (O) conformations given top right below template name. Data presentation as described in Figure 3.

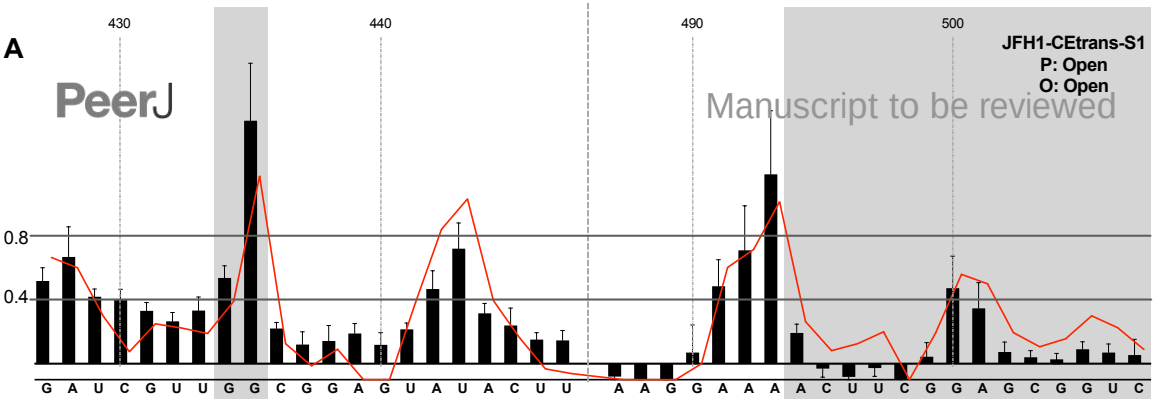

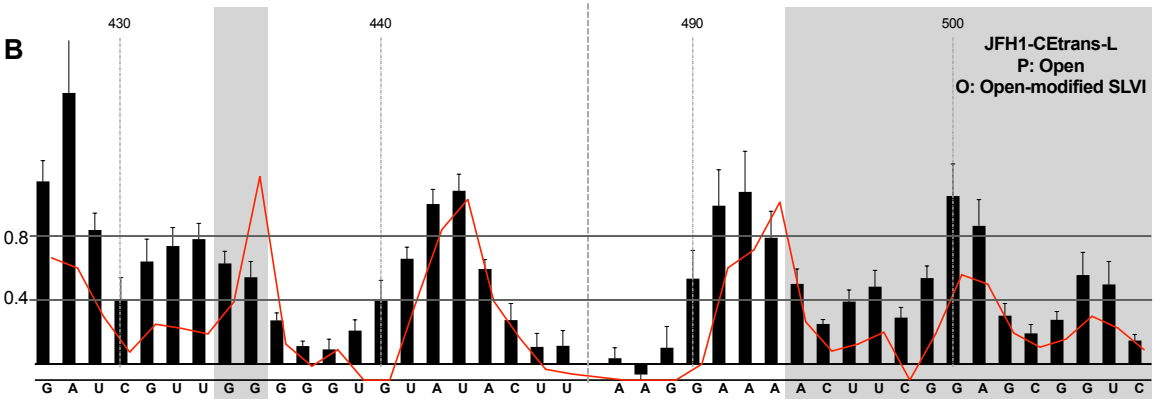

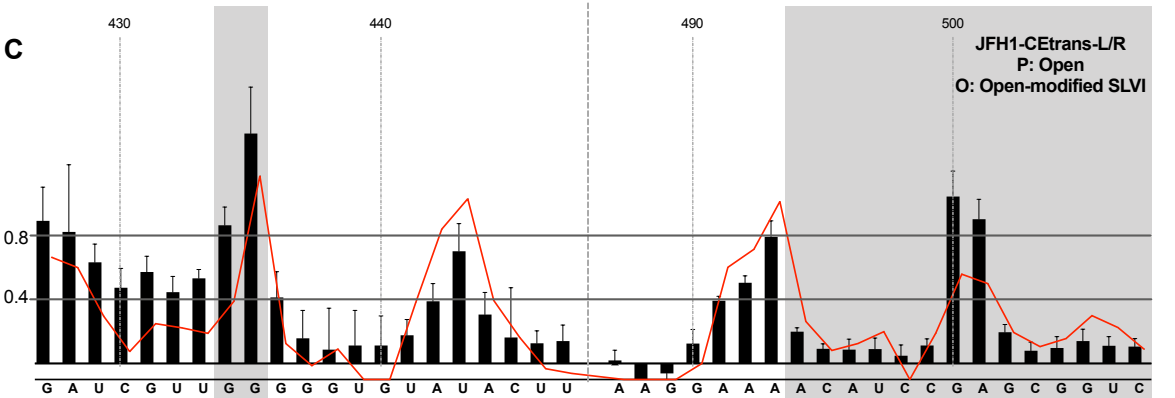

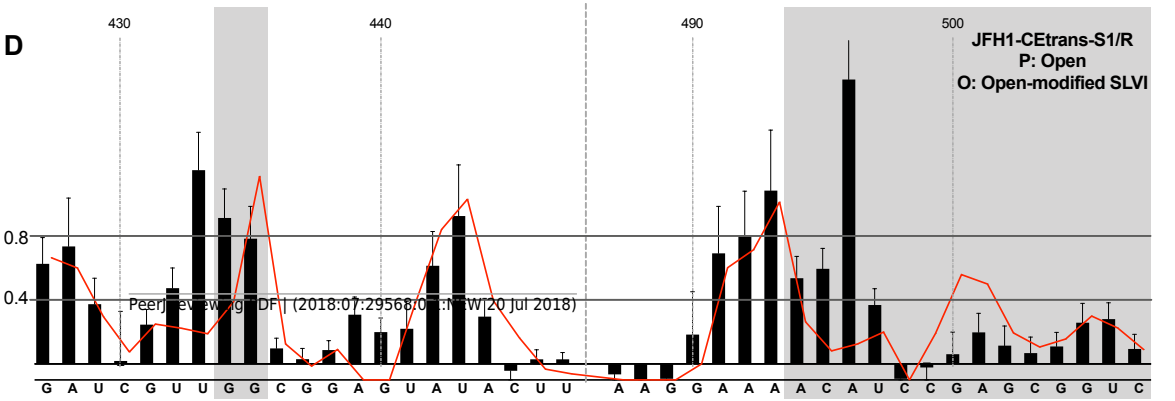

Figure 5(on next page)

SHAPE analysis of S1 and SLVI mutants with predicted ‘closed’ conformation.

SHAPE reactivities are shown for (A) JFH1-CEtrans-S1/L, (B) JFH1-CEtrans-R, and (C) JFH1-CEtrans-S1/L/R, with predicted (P) and observed (O) conformations given top right below template name. Data presentation as described in Figure 3.

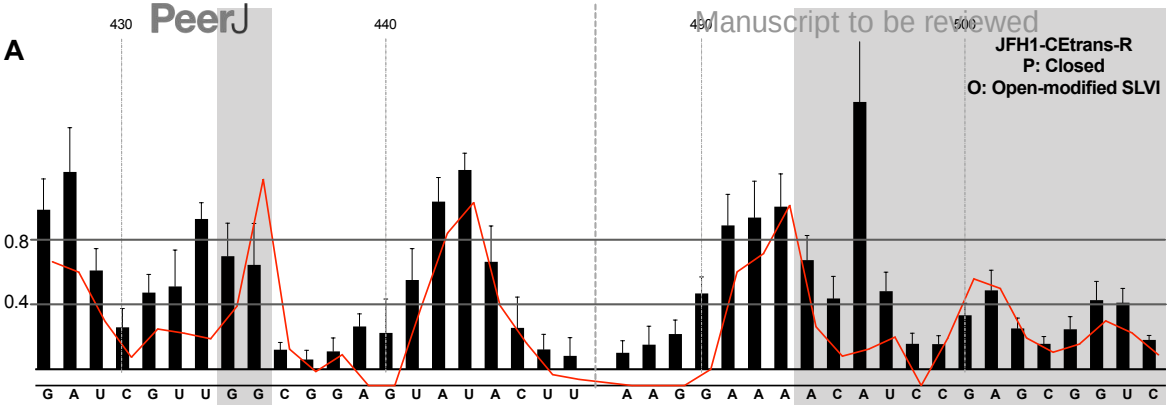

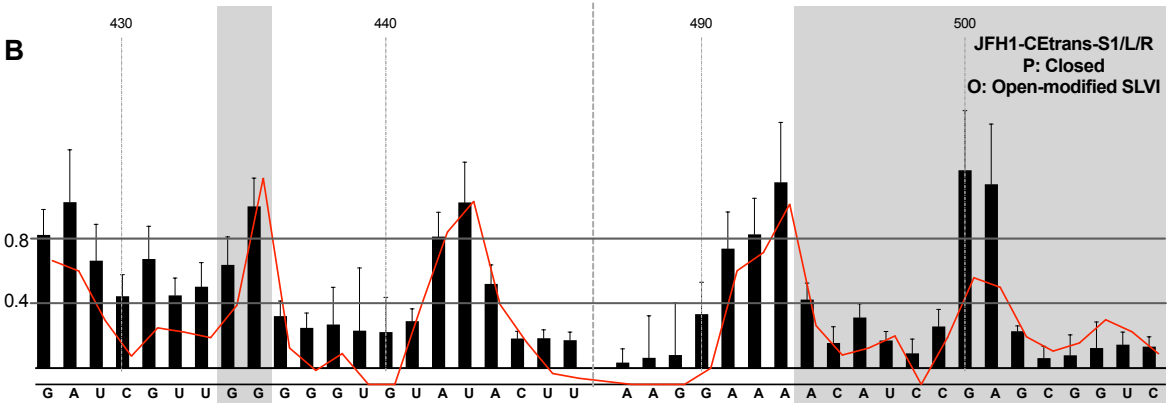

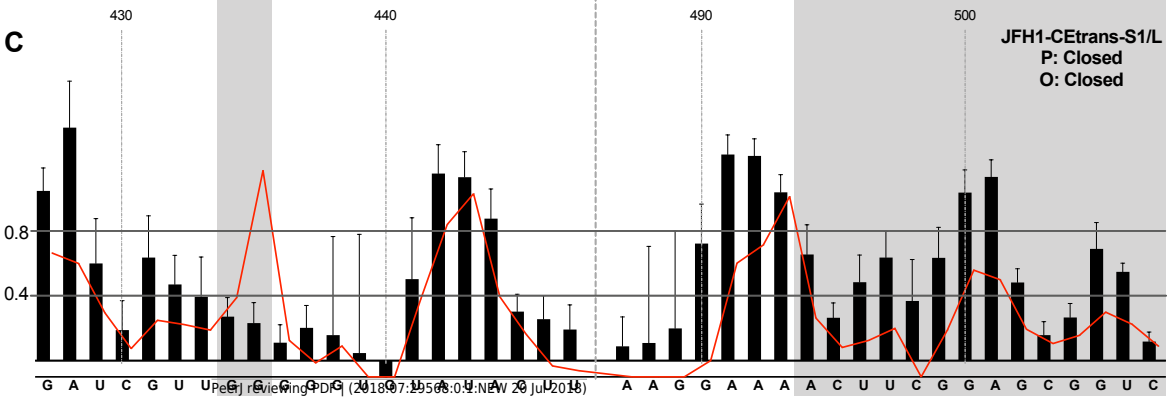

Figure 6(on next page)

Phenotypic characterisation of JFH-1 reporter bearing S1 and SLVI mutations.

Translation levels were determined by luciferase assay for (A) JFH1-luc-trans:ΔNS5B and JFH1-CEtrans, (B) JFH1-CEtrans, S1 and SLVI mutants, and (C) JFH1-luc-trans:ΔNS5B and JFH1-CEtrans in HeLa cells. Cell lysates were harvested at 4 h and luciferase readings calculated as a ratio of Firefly luciferase to a co-transfected Renilla luciferase control RNA. Replication kinetics of (D) JFH1-CErep, S1 and SLVI mutants, and (E) JFH1-CErep-S1 supplemented with S1-miR122, were determined by luciferase assays at 4, 21, 28, and 45h post-transfection. Luciferase readings are expressed as a percentage of the 4 h reading to normalise against translation of input RNA. A polymerase active site mutant, GDD to GNN, was included as replication control (Pol –ve). For all assays error bars represent SD of 3 replicate transfections from triplicate experiments, with statistical significance calculated by unpaired t-test analysis using GraphPad Prism V7.

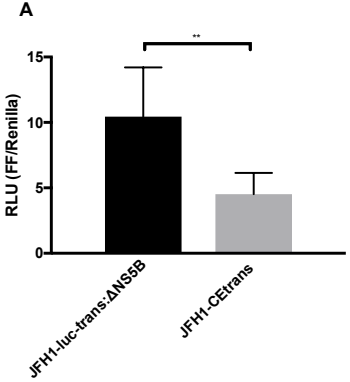
A
**
RLU (FF/Renilla)
15
10
5
0
JFH1-luc-trans:ΔNS5B
JFH1-CEtrans

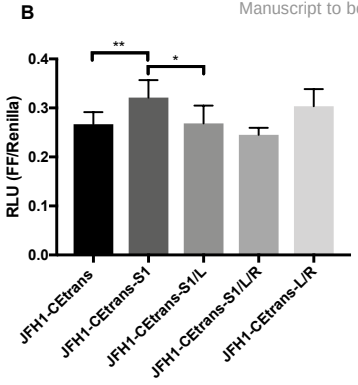
B
**
*
RLU (FF/Renilla)
0.4
0.3
0.2
0.1
0.0
JFH1-CEtrans
JFH1-CEtrans-S1
JFH1-CEtrans-S1/L
JFH1-CEtrans-S1/L/R
JFH1-CEtrans-L/R

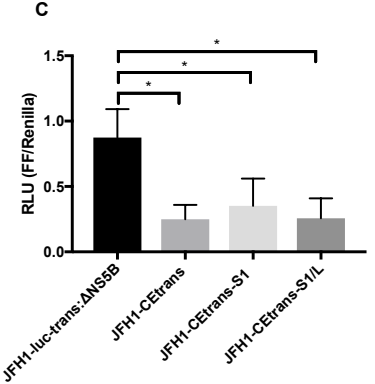
C
*
*
*
RLU (FF/Renilla)
1.5
1.0
0.5
0.0
JFH1-luc-trans:ΔNS5B
JFH1-CEtrans
JFH1-CEtrans-S1
JFH1-CEtrans-S1/L

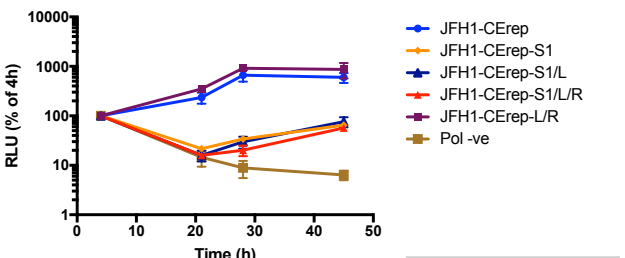
D
RLU (% of 4h)
10000
1000
100
10
1
0
10
20
30
40
50
Time (h)
JFH1-CErep
JFH1-CErep-S1
JFH1-CErep-S1/L
JFH1-CErep-S1/L/R
JFH1-CErep-L/R
Pol -ve

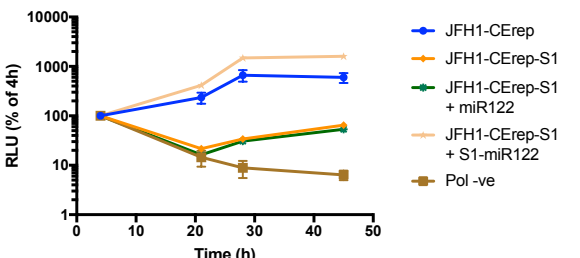
E
RLU (% of 4h)
10000
1000
100
10
1
0
10
20
30
40
50
Time (h)
JFH1-CErep
JFH1-CErep-S1
JFH1-CErep-S1
+ miR122
JFH1-CErep-S1
+ S1-miR122
Pol -ve

Table 1(on next page)

Substitutions and predicted conformations

Table 1 – Substitutions and predicted conformations

Mutant	Mutations	Predicted Conformation[a]
Parental JFH1-CEtrans or JFH1-CErep	n/a	Open
JFH1-CEtrans-L / JFH1-CErep-L	$C_{436}G$, $A_{439}U$	Open
JFH1-CEtrans-R / JFH1-CErep-R	$U_{496}A$, $G_{499}C$	Closed
JFH1-CEtrans-L/R / JFH1-CErep-L/R	$C_{436}G$, $A_{439}U$, $U_{496}A$, $G_{499}C$	Open
JFH1-CEtrans-S1 / JFH1-CErep-S1	$U_{25}A$, $G_{28}C$	Open
JFH1-CEtrans-S1/L / JFH1-CErep-S1/L	$U_{25}A$, $G_{28}C$, $C_{436}G$, $A_{439}U$	Closed
JFH1-CEtrans-S1/R / JFH1-CErep-S1/R	$U_{25}A$, $G_{28}C$, $U_{496}A$, $G_{499}C$	Open
JFH1-CEtrans-S1/L/R / JFH1-CErep-S1/L/R	$U_{25}A$, $G_{28}C$, $C_{436}G$, $A_{439}U$, $U_{496}A$, $G_{499}C$	Closed

[a] in the presence of miR122